Advances in Atmospheric Sciences
Impact Factor: 3.158
E-alert
ISSN 0256-1530
CN 11-1925/O4

An Observational Study on the Local Climate Effect of the Shangyi Wind Farm in Hebei Province

Yonghong LIU, Bing DANG, Yongming XU, Fuzhong WENG

Citation: Liu, Y. H., B. Dang, Y. M. Xu, F. Z. Weng, 2021: An Observational Study on the Local Climate Effect of the Shangyi Wind Farm in Hebei Province, *Adv. Atmos. Sci.*, In press. doi: 10.1007/s00376-021-0290-0.

View online: https://doi.org/10.1007/s00376-021-0290-0

ADVANCES IN ATMOSPHERIC SCIENCES, VOL. 38, NOVEMBER 2021, 1905–1919

• **Original Paper** •

An Observational Study on the Local Climate Effect of the Shangyi Wind Farm in Hebei Province

Yonghong LIU*[1], Bing DANG[2], Yongming XU[3], and Fuzhong WENG[1]

[1]*State Key Laboratory of Severe Weather*, *Chinese Academy of Meteorological Sciences*, *Beijing* 100081, *China*

[2]*Beijing Municipal Climate Center*, *Beijing* 100089, *China*

[3]*School of Remote Sensing and Geomatics Engineering*, *Nanjing University of Information Science and Technology*, *Nanjing* 21004, *China*

(Received 17 September 2020; revised 6 June 2021; accepted 8 June 2021)

ABSTRACT

Zhangjiakou is an important wind power base in Hebei Province, China. The impact of its wind farms on the local climate is controversial. Based on long-term meteorological data from 1981 to 2018, we investigated the effects of the Shangyi Wind Farm (SWF) in Zhangjiakou on air temperature, wind speed, relative humidity, and precipitation using the anomaly or ratio method between the impacted weather station and the non-impacted background weather station. The influence of the SWF on land surface temperature (LST) and evapotranspiration (ET) using MODIS satellite data from 2003 to 2018 was also explored. The results showed that the SWF had an atmospheric warming effect at night especially in summer and autumn (up to 0.95°C). The daytime air temperature changes were marginal, and their signs were varying depending on the season. The annual mean wind speed decreased by 6%, mainly noted in spring and winter (up to 14%). The precipitation and relative humidity were not affected by the SWF. There was no increase in LST in the SWF perhaps due to the increased vegetation coverage unrelated to the wind farms, which canceled out the wind farm-induced land surface warming and also resulted in an increase in ET. The results showed that the impact of wind farms on the local climate was significant, while their impact on the regional climate was slight.

Key words: wind farms, local climate effect, air temperature, wind speed, land surface temperature, evapotranspiration

Citation: Liu, Y. H., B. Dang, Y. M. Xu, and F. Z. Weng, 2021: An observational study on the local climate effect of the Shangyi Wind Farm in Hebei Province. *Adv. Atmos. Sci.*, **38**(11), 1905–1919, https://doi.org/10.1007/s00376-021-0290-0.

Article Highlights:

- Meteorological observations confirmed that the SWF had a significant local atmospheric heating effect especially at night and a wind speed reduction effect.
- Satellite observations showed that the SWF had no increase in LST perhaps due to the increased NDVI unrelated to wind farms.
- The impact of the SWF on the regional climate is slight.

1. Introduction

Wind power is a new, renewable, and clean energy resource that has great potential for development, well-established techniques, and the advantage of large-scale application (Leung et al., 2012). The wind power installed capacity has been continuously growing since the 1990s. According to the Global Wind Energy Council (GWEC, 2020), the installed global wind power capacity increased by 60.4 GW in 2019, corresponding to a 19% increase over 2018. With the large-scale development of wind power around the globe, more attention has been drawn to the impact of the arrangement and operation of large-scale wind farms on ecosystems and the climate (Zhao et al., 2011; Li et al., 2018; Jiang et al., 2019).

Existing research results have shown that the operation of wind farms mainly affects the climate from the following three aspects. (1) The rotation of wind turbines converts wind power to electrical power and turbulent power, thus changing the original natural energy circulation pattern and in turn the surface drag coefficient (Roy and Traiteur, 2010). (2) The construction of wind farms could alter the surface roughness and lead to variations in heat exchange between the land surface and atmosphere (Abbasi et al.,

* Corresponding author: Yonghong LIU
Email: lyh7414@163.com

2016), which could affect the local climate. (3) The rotation of wind turbine blades disturbs the air and thus increases the intensity of the turbulence occurring in the atmospheric boundary layer (Xia et al., 2016). This process alters the original surface fluxes and indirectly affects the meteorological conditions. Thus, wind farms can alter both the local meteorological conditions and heat exchange between the land surface and the atmosphere. In particular, the impact of wind farms on air temperature, wind speed, land surface temperature (LST), and evapotranspiration (ET) has received wide attention (Roy, 2004; Zhou et al., 2012; Vautard et al., 2014; Armstrong et al., 2016).

Studies on the local climate effects of wind farms have mainly adopted three methods, including meteorological observations (Rajewski et al., 2013; Smith et al., 2013; Xu, 2014), satellite remote sensing (Christiansen and Hasager, 2005; Walsh-Thomas et al., 2012; Zhou et al., 2013a; Harris et al., 2014), and numerical simulations (Frandsen et al., 2009; Roy, 2011; Cervarich, 2013; Fitch, 2015). Meteorological observations of wind farms consist of in situ meteorological observations and historical meteorological observations because variations in meteorological observation factors can directly reflect the effect of wind farms on climate. However, given the limited availability and high cost of in situ observational data, which usually spans only a few months, the effects of climate variations and interannual fluctuations cannot be thoroughly eliminated from these data. Comparisons and analyses of historical meteorological observations require a sufficiently long data collection period with data collected at suitable and representative meteorological stations that are located outside of the impact range of wind farms. The quality of the observational data also needs to be strictly controlled because (1) the local climate effect of wind farms is usually small, barely exceeding the interannual natural variability of the local climate in most cases (Chen, 2018) and (2) the construction sites of wind farms are usually far from the meteorological stations. Because of these limitations, very few studies on the effect of wind farms on climate have adopted meteorological observations.

In comparison, satellite remote sensing data are inexpensive and can be used to identify the effect of wind farms on climate on larger temporal and spatial scales. Thus far, the included observational factors lack diversity and are mainly composed of the LST and ET (Zhou et al., 2013a, b; Li, 2016). Given the constraint of limited observational data, numerical simulations have been the dominant method of investigating the climate effect of wind farms because of the diversity of the output climate factors and their ability to explain the mechanisms of the local climate effect of wind fields (Roy, 2011; Fitch et al., 2013). The limitation of this method lies in the fact that there are uncertainties in numerical models and the design of wind farm simulation experiments; as a result, the verification of the simulation results is a complex task. Thus, uncertain and controversial simulation results have been published (Wang and Prinn, 2009; Vautard et al., 2014; Fitch, 2015).

In the last 10 years, the number of studies on the climate effect of large-scale wind farms in China has been gradually increasing. Studies based on numerical simulations have shown the following. (1) After the construction of large-scale wind farms in the Hexi Corridor area in China, the average wind speed was reduced by 0.3 m s^{-1}. In addition, in the low atmosphere over the wind farms and their downstream areas, the air temperature rose by up to 0.3°C and the specific humidity decreased by 0.2 g kg^{-1} (Hu, 2012; Hu and Wang, 2018). (2) The construction of large-scale wind farms in China can result in ±0.5 K variations in the 2-m air temperature and ±30 m^2 s^{-2} variance in wind speed (Sun, 2018). In situ meteorological observation experiments have shown that wind farms in Inner Mongolia increased the air temperature and lowered the humidity in the atmosphere less than 3 m above the ground surface (Xu, 2014). In addition, satellite remote sensing observations have shown that (1) in the eight years after the construction of large-scale wind farms in Guazhou, Gansu Province, the nighttime LST values in summer, autumn, and winter rose by 0.51°C, 0.48°C, and 0.38°C, respectively (Chang et al., 2016); and (2) wind farms in Inner Mongolia increased the local surface ET (Li, 2016). However, these studies were mainly focused on arid areas with sparse vegetation in North China, and few such studies exist in semiarid or humid areas in South China. Thus far, the only existing research is a case study on the local climate effect of the Dabie Mountains Wind Farm in Hubei Province based on meteorological observations (Zhang et al., 2019).

Zhangjiakou, Hebei Province, is a semiarid area and an important wind power base in China. With a continuous increase in installed wind power capacity in recent years, it has generated much controversy regarding the climatic impact of wind farms in Zhangjiakou. Zhu (2014) concluded that the development of wind farms in northern Hebei had no significant influence on the diffusion of air pollutants in the Beijing–Tianjin–Hebei region. Later, based on 24 years of meteorological data, Yan et al. (2015) showed that the wind speed in Zhangjiakou was not lowered as a result of the construction of large-scale wind farms. Based on wind speed data from meteorological stations in Zhangjiakou, Huo et al. (2015) further showed that there was no significant correlation between the wind power installed capacity and wind speed. In contrast, Li et al. (2015) found that instead of lowering the local wind speed, the increased wind power installed capacity in Zhangjiakou resulted in a gradually increasing wind speed. However, these studies did not consider whether the meteorological stations were within the influence range of the wind farms. In addition to changes in underlying surface conditions, changes in local climate factors are also affected by interannual changes and climate changes, and these studies have given less consideration to how to separate these factors. Therefore, it is difficult to determine whether changes in local weather conditions are truly affected by wind farms.

Given the discrepant conclusions in the literature, we chose the Shangyi Wind Farm (SWF) in Zhangjiakou for this study and adopted the methods of meteorological observa-

tions and remote sensing to investigate the impact of the wind farms on the local climate. Several factors, including underlying surface conditions, interannual changes in meteorological elements, and climate change, were also considered. On this basis, we will discuss the local climate effect of wind farms in semiarid areas in China and their possible influences on regional climate change to provide a relevant reference and basis for assessing the impact of the construction of large-scale wind farms on the regional environment.

The paper is organized as follow: 1) section 2 introduces the general situation of the wind farms in the study area and the meteorological data and satellite data used; 2) section 3 presents the meteorological methods and satellite remote sensing methods used in the local climate effect assessment of wind farms; 3) section 4 is the results of local climate effects of wind farms; 4) section 5 discusses the impact of vegetation coverage on the local climate effect, the comparison between the local climate effect of wind farms and the regional climate change and some uncertainties; 5) section 6 is the conclusion.

2. Research area and data

2.1. *Study Area*

The research area is in Shangyi County, Zhangjiakou, Hebei Province, China (40.77°–41.54°N, 113.48°–114.35°E), as shown in Fig. 1. From 2009 to the end of 2015, 272 wind turbines were installed at the SWF. The hub height of the

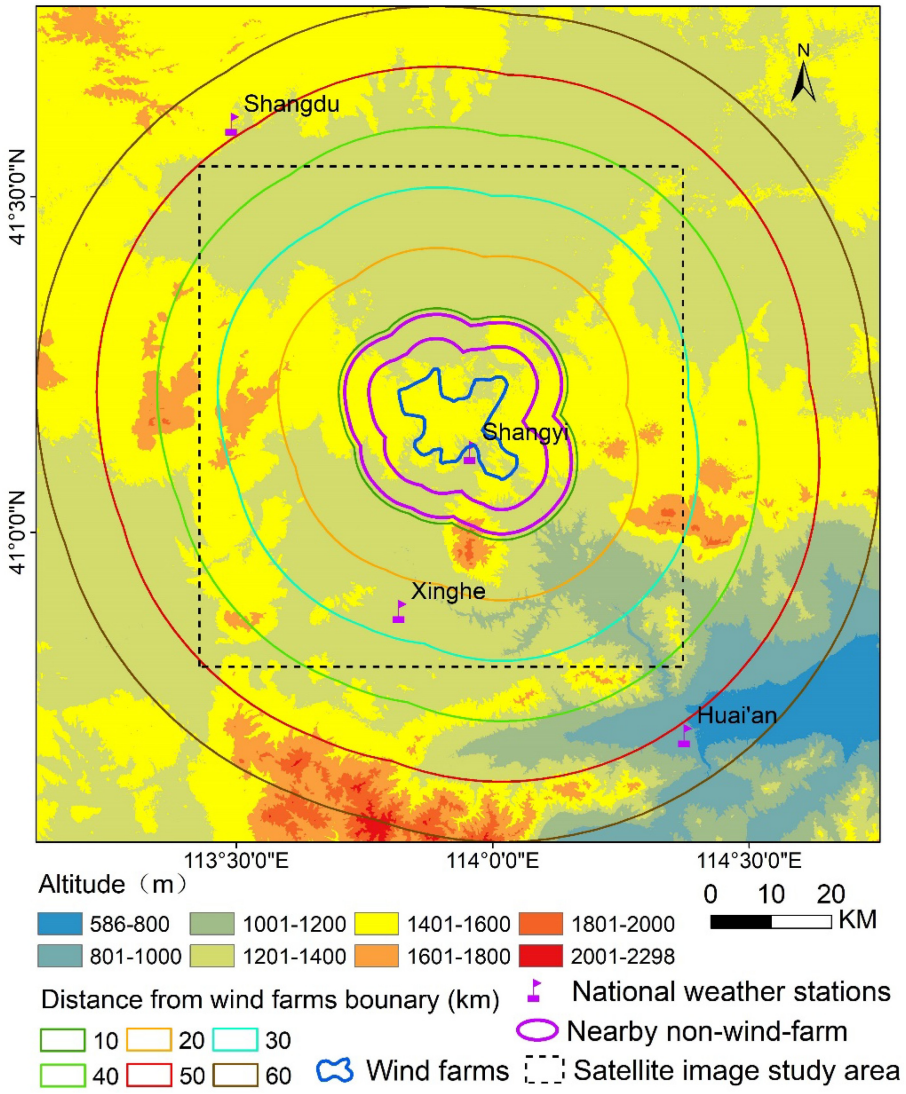

Fig. 1. Geographic map of the location and surrounding areas of the SWF in Zhangjiakou, Hebei Province. The boundary of the SWF is denoted by a dark blue line, and the surrounding non-impacted area (Nearby non-wind-farm, 5–9 km away from the wind farms boundary line) corresponds to the area between the purple lines. Within 60 km from the boundary of the wind farms, there are four national meteorological stations, including Shangyi (SY), Xinghe (XH), Huai'an (HA), and Shangdu (SD) stations.

wind turbines is 65–90 m, and the total installed capacity is 450 MW, with a distributed area of approximately 200 km^2. The region where the wind farms are located belongs to a semiarid continental monsoon climate region with an altitude of 1375–1573 m. The natural vegetation is dominated by herbaceous plants, and small areas of forests, farmlands, and shrubs are sparsely distributed in valleys and on gentle slopes. The average annual precipitation is 414 mm and the direction of the predominant wind is NW followed by WSW.

Within 60 km of the wind farms in the research area, there are four national meteorological stations: Shangyi (SY), Shangdu (SD), Huai'an (HA), and Xinghe (XH) (Fig. 1). The SY meteorological station lies closest to the wind farms and can therefore be used to assess the local climate effect of the wind farms. The SD station is 50 km from the wind farms and upstream considering the dominant wind (NW). The HA station is 52 km from the wind farms in the downstream direction, again considering the dominant wind (NW). In contrast, the XH station is 27 km southwest of the wind farms. The satellite image study area is an area within around 40 km of the center of the wind farms, which represents an area of about 6400 km^2.

2.2. *Data*

The National Meteorological Information Center provided the meteorological data, including homogenized monthly mean air temperature, maximum air temperature, minimum air temperature, average wind speed, average relative humidity, 0200 and 1400 local time (LT) air temperature and relative humidity during 1981–2018 from the SY and HA national meteorological stations in Hebei Province and the XH and SD national meteorological stations in Inner Mongolia. Homogenized meteorological data can eliminate the effects of artifacts caused by environmental, equipment, and human factors on observed data. As a result, homogenized data can more reliably reflect the true characteristics of the elements of climate change.

The satellite data included the LST, land surface ET, and normalized difference vegetation index (NDVI) data in the sixth version of the Moderate Resolution Imaging Spectroradiometer (MODIS) Terra satellite (MOD*) and Aqua satellite products (MYD*) from the National Aeronautics and Space Administration (NASA) (Wan, 2008; Mu, et al., 2011) for analyzing the LST and ET at the local wind farms. The Terra satellite passes over this area at approximately 1030 and 2200 LT, and the Aqua satellite passes at approximately 1330 and 0130 LT. Because MODIS/Aqua data are available only starting from July 2002, we chose the LST data at 1 km resolution synthesized over eight days (MOD11A2 and MYD11A2), the ET data at 500 m resolution synthesized over eight days (MOD16A2 and MYD16A2), and the NDVI product at 250 m resolution synthesized over 16 days (MOD13Q1 and MYD13Q1) during 2003–18.

For the LST images, we adopted the effective pixel mean to calculate the annual, seasonal, daytime (including approximately 1030 and 1330 LT) and nighttime (including approximately 2230 and approximately 0130 LT) LST values based on the Terra and Aqua satellite data. For the ET images, we adopted the effective pixel accumulation value to calculate the annual and seasonal total ET values based on using both sets of satellite data. The two sets of satellite data were then averaged to yield the final result. For the NDVI, we adopted the effective pixel mean to calculate the annual mean NDVI, and the average of the two sets of satellite data represents the annual mean NDVI.

In this study, spring was defined as March to May, summer as June to August, autumn as September to November, and winter as December to February.

3. Methods

3.1. *Background meteorological station*

In addition to possible effects from the wind farms of interest, variations in meteorological factors at the chosen meteorological stations can also be influenced by fluctuations related to the interannual variability of meteorological conditions and climate change. It is impossible to determine the independent effect of the wind farms based on one meteorological station. Thus, we had to compare the chosen research stations with a background station located outside the range of influence of the wind farms to eliminate the effects of interannual fluctuations and climate change. Choosing a suitable background station was the key to assessing variations in meteorological factors in the local wind farms.

The background station had to be similar to the research station in climate type and geographic condition and subject to no influence by the wind farms. Numerical simulations showed that the wind speed can be reduced in areas 30–60 km downstream of a wind farm (Frandsen et al., 2009). Thus, the background station had to be at least 30 km from the wind farm. Here, we analyzed the similarities in the climate factors and geological conditions between the SY station and other national meteorological stations, including HA, SD, and XH, before the construction of these wind farms (1981–2008). The results are shown in Fig. 2.

Figure 2a shows that the SY and SD stations had the highest correlation coefficients for average air temperature, wind speed, and relative humidity. The correlation coefficients are 0.99, 0.75, and 0.58, respectively. The two stations also have the smallest difference in altitude (only 44 m) and are more than 30 km apart (Fig. 2b). Moreover, the SD station is in the upstream area along the dominant wind direction in this area. Thus, the SD station was chosen as the background station for analyzing the local climate effect of the wind farms.

3.2. *Quantification of the local climate effects of the wind farms*

To maintain consistency with the satellite observational times, we chose 2003–08 as the preimpact period before the wind farms were built and 2016–18 as the postim-

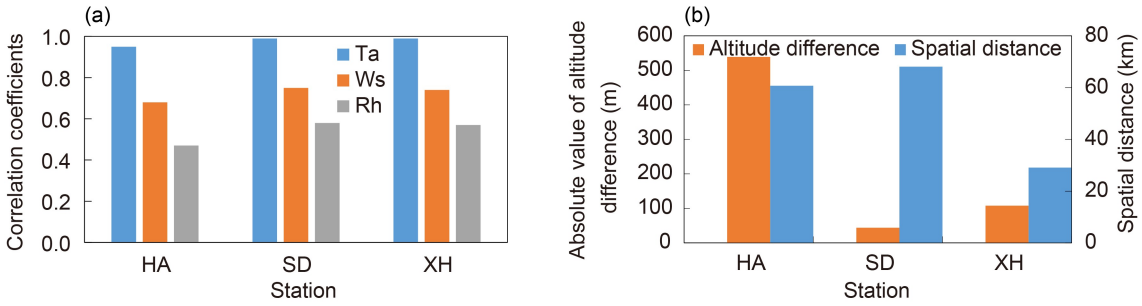

Fig. 2. Correlations in climate factors (a) and geological differences (b) between the SY station and other national meteorological stations (HA, SD, and XH). Ta is the annual mean temperature, and Ws is the annual mean wind speed, and Rh is the annual mean relative humidity. The region where the SY station is located belongs to a semiarid continental monsoon climate region with an altitude of 1375–1573 m. The average precipitation at the SY meteorological station is 414 mm, and over the entire year, the direction of the predominant wind is NW followed by WSW.

pact period after the wind farms were built. On this basis, we further defined the following parameters to quantify the effects of the wind farms on the air temperature (T), wind speed (W), relative humidity (H), and precipitation (P):

$$\mathrm{DT} = T_{\mathrm{SY}} - T_{\mathrm{SD}}\,, \tag{1}$$

$$\Delta T = \mathrm{DT}_{\mathrm{AF}} - \mathrm{DT}_{\mathrm{BF}}\,, \tag{2}$$

$$\mathrm{rW} = W_{\mathrm{SY}}/W_{\mathrm{SD}}\,, \tag{3}$$

$$\Delta\mathrm{rW} = \mathrm{rW}_{\mathrm{AF}} - \mathrm{rW}_{\mathrm{BF}}\,, \tag{4}$$

$$\mathrm{rH} = H_{\mathrm{SY}}/H_{\mathrm{SD}}\,, \tag{5}$$

$$\Delta\mathrm{rH} = \mathrm{rH}_{\mathrm{AF}} - \mathrm{rH}_{\mathrm{BF}}\,, \tag{6}$$

$$\mathrm{rP} = P_{\mathrm{SY}}/P_{\mathrm{SD}}\,, \tag{7}$$

$$\Delta\mathrm{rP} = \mathrm{rP}_{\mathrm{AF}} - \mathrm{rP}_{\mathrm{BF}}\,, \tag{8}$$

where DT (units: °C) represents the difference in air temperature between the SY (T_{SY}) and SD (T_{SD}) stations, rW represents the wind speed ratio between the SY (W_{SY}) and SD (W_{SD}) stations, rH represents the relative humidity ratio between the SY (H_{SY}) and SD (H_{SD}) stations, and rP represents the precipitation ratio between the SY (P_{SY}) and SD (P_{SD}) stations. ΔT (units: °C) represents the air temperature change after the wind farms were built ($\mathrm{DT}_{\mathrm{AF}}$) relative to before ($\mathrm{DT}_{\mathrm{BF}}$), and ΔrW represents the wind speed change after the wind farms were built ($\mathrm{rW}_{\mathrm{AF}}$) compared to before ($\mathrm{rW}_{\mathrm{BF}}$), and ΔrH represents the relative humidity change after the wind farms were built ($\mathrm{rH}_{\mathrm{AF}}$) compared to before ($\mathrm{rH}_{\mathrm{BF}}$), and ΔrP represents the precipitation change after the wind farms were built ($\mathrm{rP}_{\mathrm{AF}}$) compared to before ($\mathrm{rP}_{\mathrm{BF}}$).

To determine whether the wind farms had a significant impact on the local air temperature and wind speed variations, a sliding t-test method was introduced to analyze abrupt changes in the time series data of air temperature, wind speed, relative humidity, and precipitation. A sliding t-test is often used for the detection of abrupt changes potentially related to climate change in time series (Wei, 2007). The basic idea of the sliding t-test method is to examine whether there is a significant difference in the means of two sub-sequences in a climate series as a question of whether there is a significant difference in the two overall means. If the difference in the mean of the two subsequences exceeds a certain level of significance, it can be considered that a mutation has occurred. In addition to climate change factors, the occurrence of abrupt changes can also be caused by non-climate change factors, such as the relocation of weather stations, changes in the surrounding environment, human activities, etc. Because the construction of the wind farms is less than 10 years old, the sliding step length was defined as five years.ed as five years.

3.3. *Assessment of the local climate effects of the wind farms based on satellite data*

3.3.1. *Regional anomaly*

To remove the interannual variations in the meteorological factors in the background area of wind farms, we processed the LST and ET satellite images to obtain their changes after the construction of the wind farms by the regional anomaly method (Zhou et al., 2013a).

$$\mathrm{AR\_LST} = \mathrm{LST} - \mathrm{LST}_{\mathrm{RM}}\,, \tag{9}$$

$$\Delta\mathrm{AR\_LST} = \mathrm{AR\_LST}_{\mathrm{AF}} - \mathrm{AR\_LST}_{\mathrm{BF}}\,, \tag{10}$$

$$\Delta\mathrm{LST} = \mathrm{LST}_{\mathrm{AF}} - \mathrm{LST}_{\mathrm{BF}}\,, \tag{11}$$

$$\mathrm{AR\_ET} = \mathrm{ET} - \mathrm{ET}_{\mathrm{RM}}\,, \tag{12}$$

$$\Delta\mathrm{AR\_ET} = \mathrm{AR\_ET}_{\mathrm{AF}} - \mathrm{AR\_ET}_{\mathrm{BF}}\,, \tag{13}$$

$$\Delta ET = ET_{AF} - ET_{BF} . \quad (14)$$

where AR_LST (or AR_ET) is the anomaly between the LST (or ET) image and the regional mean value (LST_{RM} or ET_{RM}). Here, the region is the satellite image study area in Fig. 1, an area of about 6400 km^2, which includes the wind farm (approximately 200 km^2) and surrounding areas. ΔAR_LST (or ΔAR_ET) represents the change in LST (or ET) image after the construction of the wind farms (AR_LST_{AF} or AR_ET_{AF} averaged over 2016–18) compared to before (AR_LST_{BF} or AR_ET_{BF} averaged over 2003–08). ΔLST (or ΔET) represents the change in LST (or ET) image after the wind farms were built that have not been processed by the regional anomaly method.

3.3.2. *Difference between impacted and non-impacted areas*

The regional anomaly method is based on image, and can only be used to illustrate variations between the regional mean and those in the wind farms location and cannot be used to quantitatively assess the local effect of the wind field of interest. To quantify the effects of the wind farms on the LST and ET, we processed the LST and ET data to obtain their changes after the construction of the wind farms by using the difference method between the impacted and non-impacted areas (Zhou et al., 2013a).

$$DLST = LST_{WF} - LST_{NWF} , \quad (15)$$

$$\Delta DLST = DLST_{AF} - DLST_{BF} , \quad (16)$$

$$DET = ET_{WF} - ET_{NWF} , \quad (17)$$

$$\Delta DET = DET_{AF} - DET_{BF} . \quad (18)$$

Here, DLST (or DET) represents the difference in the average LST (or ET) between the wind farms (LST_{WF} or ET_{WF}) and the non-impacted area (LST_{NWF} or ET_{NWF}). ΔDLST (or ΔDET) represents the LST (or ET) change after the wind farms were built ($DLST_{AF}$ or DET_{AF} averaged over 2016–18) compared to before ($DLST_{BF}$ or DET_{BF} averaged over 2003–08). Here, the impacted area is where the wind farms are located, and the non-impacted area is 5–9 km away from the wind farms boundary (as shown in Fig. 1).

4. Results

4.1. *Variation in the main meteorological factors before and after the construction of the wind farms*

Regarding the temporal variation in air temperature (Figs. 3a–c), the annual mean air temperature (Ta), maximum air temperature (Tmax), and minimum air temperature (Tmin) at both the SY and SD stations showed consistent fluctuations from 1981 to 2018 and the values had not changed significantly after the wind farms appeared (2009–18), which were all within the interannual range of air temperature fluctuations before the construction of the wind farm (1981–2008). However, based upon the differences between the SY and SD stations after 2013, the mean air temperature anomaly (DTa) in 2014–18 was higher than in any year during 1989–2013, the minimum air temperature anomaly (DTmin) in 2014–18 was higher than in any year during 1981–2013, and the maximum air temperature anomaly (DTmax) in 2014–18 was not high compared to 1981–2013, which indicated that after 2013, the Ta and Tmin at the SY station were likely affected by the wind farms, although there is still some uncertainty for Ta because the DTa was also large in the early 1980s (Fig. 3a). In addition, from the sliding average *t*-test of the difference in the Ta, Tmax, Tmin between the SY and SD stations during 1981–2018 (Fig. 4a), the DTa and DTmin both had abrupt change points in 2013, and the DTmax had no abrupt change point after 2000, which indicated that after 2013, the Ta and Tmin changed significantly, while the Tmax did not change significantly. This further showed that the average air temperature and minimum air temperature at the SY station were very likely to be affected by the wind farms.

Regarding the temporal variation in the annual mean wind speed (Fig. 3d), the annual wind speed (*W*) variations at the SY and SD stations from 1981 to 2018 were consistent, and the *W* after the wind farms appeared (2009–18) did not change significantly and was still within the interannual range of wind speed changes before the construction of the wind farm (1981–2008). However, the wind speed ratio (rW) between the SY and SD stations show that after 2013 (Fig. 3d), the rW decreased significantly (during 2014–18) and was lower than any year during 2005–13 which indicates that the W at the SY station was probably affected by the wind farms, noting a degree of uncertainty since rW was also lower during 1997–2003 than any year during 2005–13. In addition, from the sliding average *t*-test of the rW between the SY and SD stations during 1981–2018 (Fig. 4b), there was one point of abrupt change in the rW in 1996 and 2013, respectively, which indicated that after 2013, the sudden change in wind speed was likely caused by the construction of wind farms. The reason for the uncertainty is that the sudden change in 1996 was not caused by wind farms.

Regarding the temporal variation in the annual mean relative humidity (Fig. 3e), the annual relative humidity (*H*) variations at the SY and SD stations were consistent, and the *H* at the SY station after the wind farms appeared (2009–18) did not change significantly and was still within the range of interannual relative humidity changes before the construction of the wind farm (1981–2008). In addition, the relative humidity ratio (rH) between the SY and SD stations show that after 2008 (Fig. 3e), the rH continuously increased during 2008–14 and dropped slightly during 2015–18, which indicated that the temporal variation may not be related to wind farms because the wind farms were built from 2009 to 2015. From the sliding average *t*-test of the rH between the SY and SD stations during 1981–2018 (Fig. 4 right), the rH

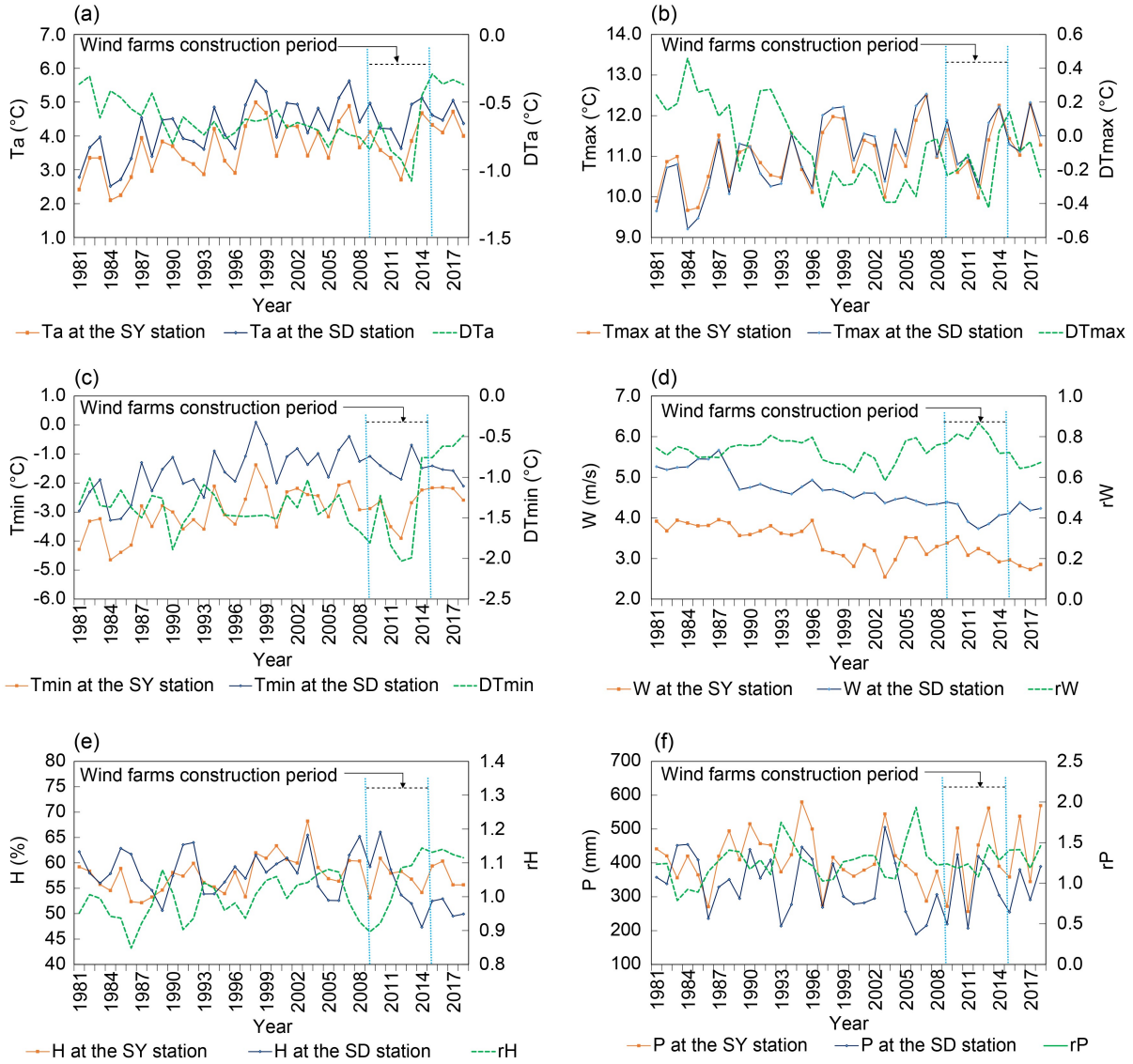

Fig. 3. Interannual variations of different local climate factors at SY and SD stations (left vertical axis) and the difference or ratio between the two stations (right vertical axis) from 1981 to 2018. The red line is the SY station and the dark blue line is the SD station. The green line is the difference (SY station minus SD station) or the ratio (SY station divided by SD station). The construction period of the wind farms is 2009–15. The following time series are shown, (a) annual mean air temperature (Ta) and the difference (DTa), (b) maximum air temperature (Tmax) and the difference (DTmax), (c) minimum air temperature (Tmin) and the difference (DTmin), (d) annual mean wind speed (*W*) and the ratio (rW), (e) annual mean relative humidity (*H*) and the ratio (rH), and (f) annual precipitation (*P*) and the ratio (rP).

exhibited three abrupt changes in 2006, 2011, and 2012, respectively, which could not determine whether or not the relative humidity was affected by the construction of wind farms.

Regarding the temporal variation in the annual precipitation (Fig. 3f), both before and after the wind farm was built, the annual variations in the precipitation (*P*) at both SY and SD stations were highly correlated, accompanied by consistent variational trends. However, because of large interannual fluctuations, no significant difference was observed between the periods before and after the construction of the wind farms. Similarly, the precipitation ratio (rP) between the SY and SD stations did not change significantly after the construction. From the sliding average *t*-test of the rP between the SY and SD stations during 1981–2018 (Fig. 4 right), the precipitation data exhibited no abrupt changes. These results indicate that the precipitation had not been affected by the wind farms.

4.2. *Possible effects of the wind farms on local meteorological factors*

The changes in DT, rW, rH, and rP after the wind farms were built in different periods are summarized in Fig. 5. To determine whether the changes are significant, their interannual standard deviations before the construction of the wind farms (1981–2008) were calculated to represent the normal

interannual fluctuations, which are also shown in Fig. 5. When the changes of different local climate factors were larger than their interannual standard deviations, the changes were considered to be statistically significant.

Figure 5a illustrates that (1) the increase in the annual mean air temperature was 0.37°C, which exceeded the interannual fluctuation (0.13°C), (2) the maximum air temperature increase was not significant (0.12°C) and was less than the interannual fluctuation (0.25°C), and (3) the minimum air temperature increase was significant (0.81°C) and was higher than the interannual fluctuation (0.19°C). These results show that the annual mean air temperature and the minimum air temperature at the SY station rose after the construction of the wind farms, while the maximum temperature had little change. Additionally, the 1400 LT air temperature showed no significant increase in any season. It decreased by 0.36°C in spring and decreased by 0.02°C in autumn and both decreases were less than the interannual fluctuation,

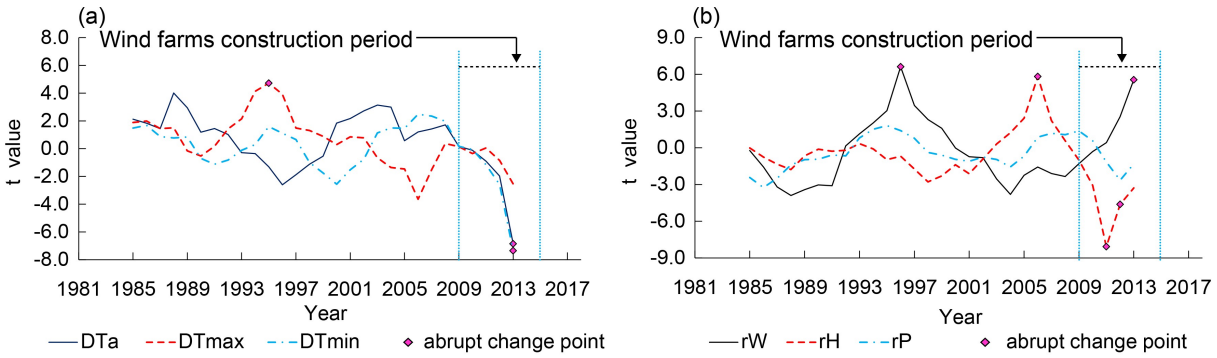

Fig. 4. Detection of abrupt changes of different climate elements based on the moving average, sliding *t*-test method from 1981 to 2018, (a) the anomaly in the annual mean air temperature (DTa), the anomaly in the maximum air temperature (DTmax), and the anomaly in the minimum air temperature (DTmin) between the SY and SD stations (b) the wind speed ratio (rW), the relative humidity ratio (rH) and the precipitation ratio (rP) between the SY and SD stations. The two orange dashed lines denote a threshold significance level of 0.01. The values outside the threshold range are abrupt change points. The construction period of the wind farms is 2009–15.

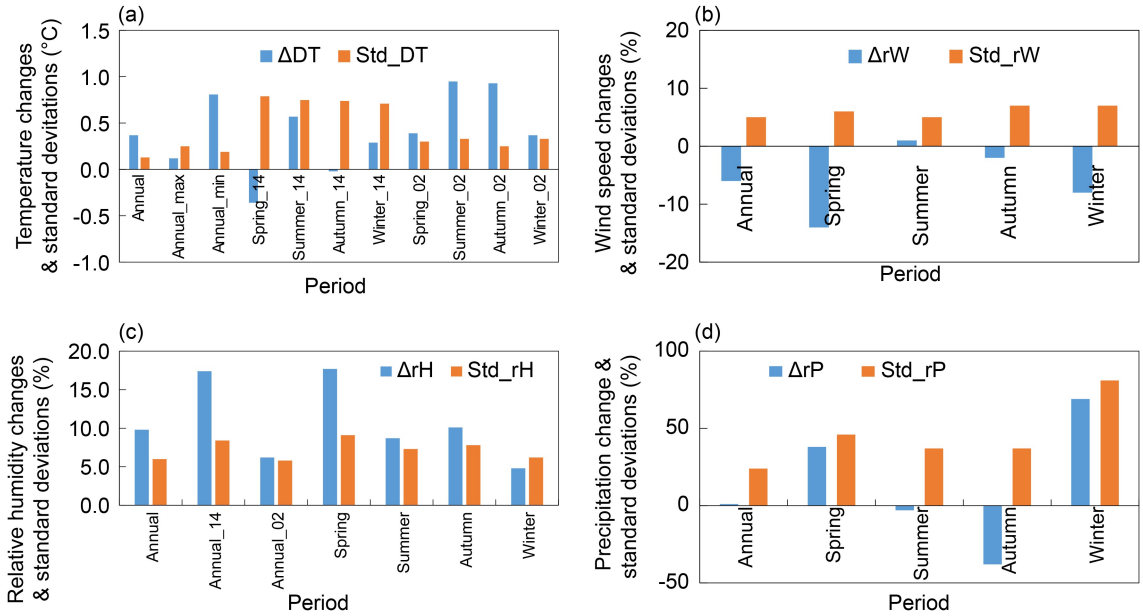

Fig. 5. Comparison of the changes of different local climate factors (a) air temperature, (b) wind speed, (c) relative humidity, and (d) precipitation) after wind farm construction for different time periods and their interannual standard deviations before the construction of the wind farms. ΔDT, ΔrW, ΔrH, and ΔrP, respectively, are the local changes in DT, rW, rH, and rP between the SY and SD stations after the construction of the wind farms, and Std_DT, Std_rW, Std_rH, and Std_rP are the interannual standard deviations of DT, rW, rH, and rP during 1981–2008, respectively, before the construction of the wind farms (Annual_max: annual maximum, Annual_min: annual minimum, Annual _14: annual mean 1400 LT, Annual _02: annual mean 0200 LT, Spring_14: 1400 LT in spring, Summer_14: 1400 LT in summer, Autumn_14: 1400 LT in autumn, Winter_14: 1400 LT in winter, Spring_02: 0200 LT in spring, Summer_02: 0200 LT in summer, Autumn_02: 0200 LT in autumn, Winter_02: 0200 LT in winter).

indicating the day-time temperature changes were marginal, and their signs were varying depending on the season. In comparison, the 0200 LT air temperature increased in all seasons, with the most significant increase (0.95°C) observed in summer and the second most significant increase (0.93°C) observed in autumn, while those in spring and winter were only 0.39°C and 0.37°C, respectively. The results show that after the wind farms were built, the air temperature rose, and the increase mainly occurred at night, especially in summer and autumn.

Regarding the wind speed (Fig. 5b), the annual mean wind speed was lowered by 6%, a value slightly larger than the interannual fluctuation (5%). The change in wind speeds of the four seasons followed the decreasing order of spring (–14%), winter (–8%), autumn (–2%), and summer (1%), among which only the changes in spring and winter exceed the interannual fluctuation. Our results thus imply that after the wind farms were built, the wind speed was lowered, and the decrease mainly occurred in spring and winter.

Regarding the relative humidity (Fig. 5c), after the wind farm was built, the annual mean relative humidity increased by 9.8%, a value larger than the interannual fluctuation (6.0%). In detail, the annual mean 1400 LT relative humidity increased significantly by 17.4%, and the relative humidity of the four seasons followed the decreasing order of spring (17.7%), autumn (10.1%), summer (8.7%), and winter (4.8%), among which only the change in winter did not exceed the interannual fluctuation. These results indicate that after the wind farm was built, the relative humidity increased.

Regarding the precipitation (Fig. 5d), after the wind farm was built, the annual mean precipitation dropped by 1%, which was significantly smaller than the interannual fluctuation (24%). The precipitation changes for the four seasons were also smaller than or close to the interannual fluctuations. Thus, after the wind farm was built, there was no significant change in precipitation.

4.3. *Possible effects of the wind farms on the LST and ET*

4.3.1. *Spatial analysis of wind farm-induced LST and ET variations*

Figure 6 shows the comparison of changes in LST (ΔLST) and the changes in LST regional anomalies (ΔAR_LST) after the wind farms were built in the research area. Regarding ΔLST, regardless of the annual average,

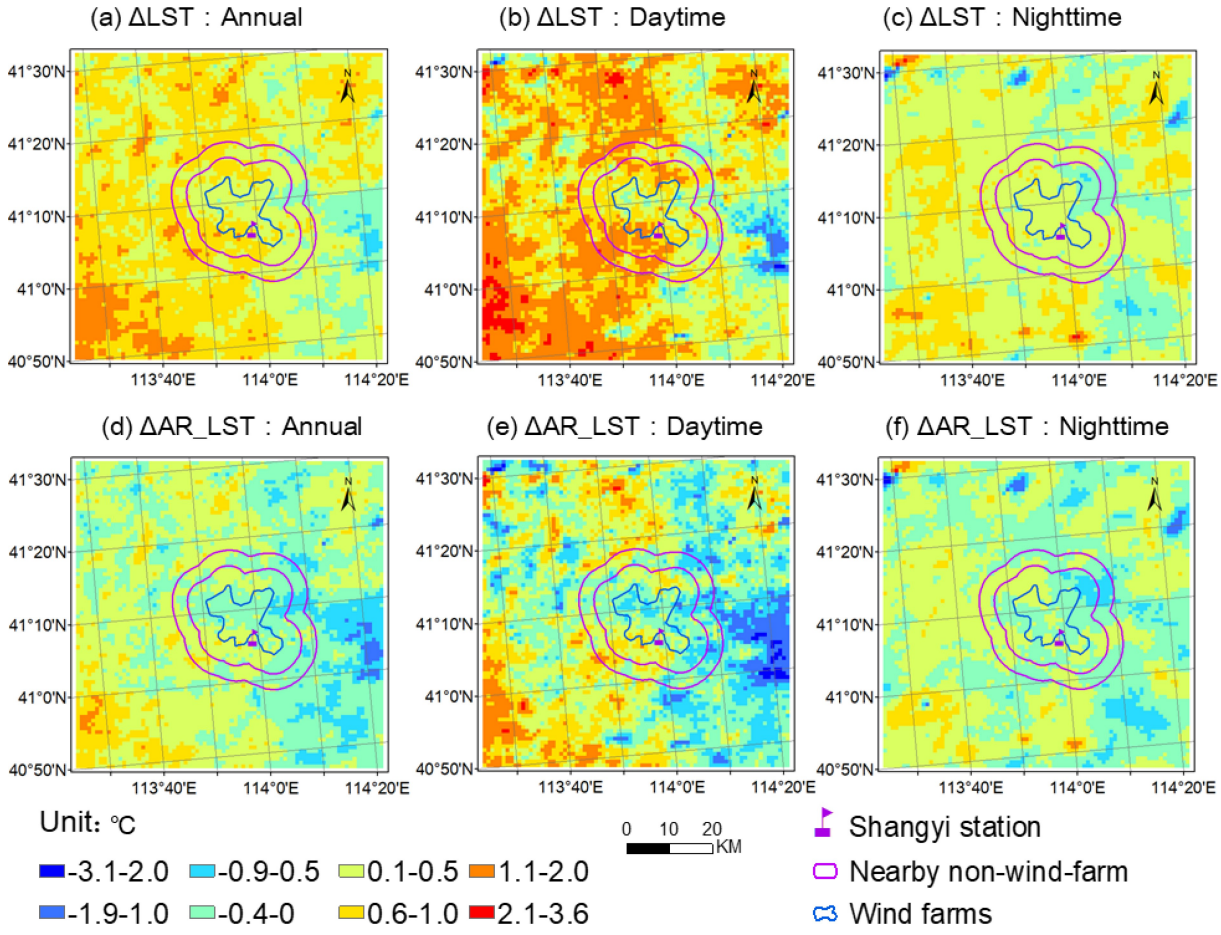

Fig. 6. Comparison of the changes in LST (ΔLST) and changes in LST regional anomalies (ΔAR_LST) in different periods after the wind farms were built (a) annual mean ΔLST, (b) annual mean daytime ΔLST, (c) annual mean nighttime ΔLST, (d) annual mean ΔAR_LST, (e) annual mean daytime ΔAR_LST, (f) annual mean nighttime ΔAR_LST.

day, and night, most areas around the wind farms showed significant increases, but the area where the wind farms are located showed only slight increases. Regarding ΔAR_LST, after processing by the regional anomaly method, the regional LST increase was significantly reduced, the area where the wind farms are located did not show a LST increase, and the average ΔAR_LST values at annual, annual mean daytime, and annual mean nighttime of the wind farms were –0.17°C, –0.05°C, and –0.11°C, respectively. This observation, characterized by a decrease, contradicts the effect of wind farms on increased LST reported in the literature (Zhou et al., 2013a; Chang et al., 2016). We will discuss the underlying mechanism later.

Figure 7 shows the comparison of changes in ET (ΔET) and changes in ET regional anomalies (ΔAR_ET) after the wind farms were built in the research area. Regarding ΔET, the ET of the wind farms and most of the surrounding areas increased both throughout the year and in summer. Regarding ΔAR_ET, after processing by the regional anomaly method, the increasing range of the regional ET was significantly reduced, and some areas of the wind farms cooled. The average ΔAR_ET values of the wind farms throughout the year and summer were 0.15 mm and 5.69 mm respectively.

4.3.2. *Effect of the wind farms on the LST and ET in the non-impacted area*

The changes in LST anomaly (ΔDLST) and the changes in ET anomaly (ΔDET) between the wind farms and the non-impacted area after the wind farms were built in different periods are summarized in Fig. 8. To determine whether the changes were significant, their interannual standard deviation (Std_DLST and Std_DET) before the construction of the wind farms (2003–2008) were calculated to represent the normal interannual fluctuations, which are shown in Fig. 8. When the changes were larger than their interannual standard deviations, the changes were considered to be statistically significant.

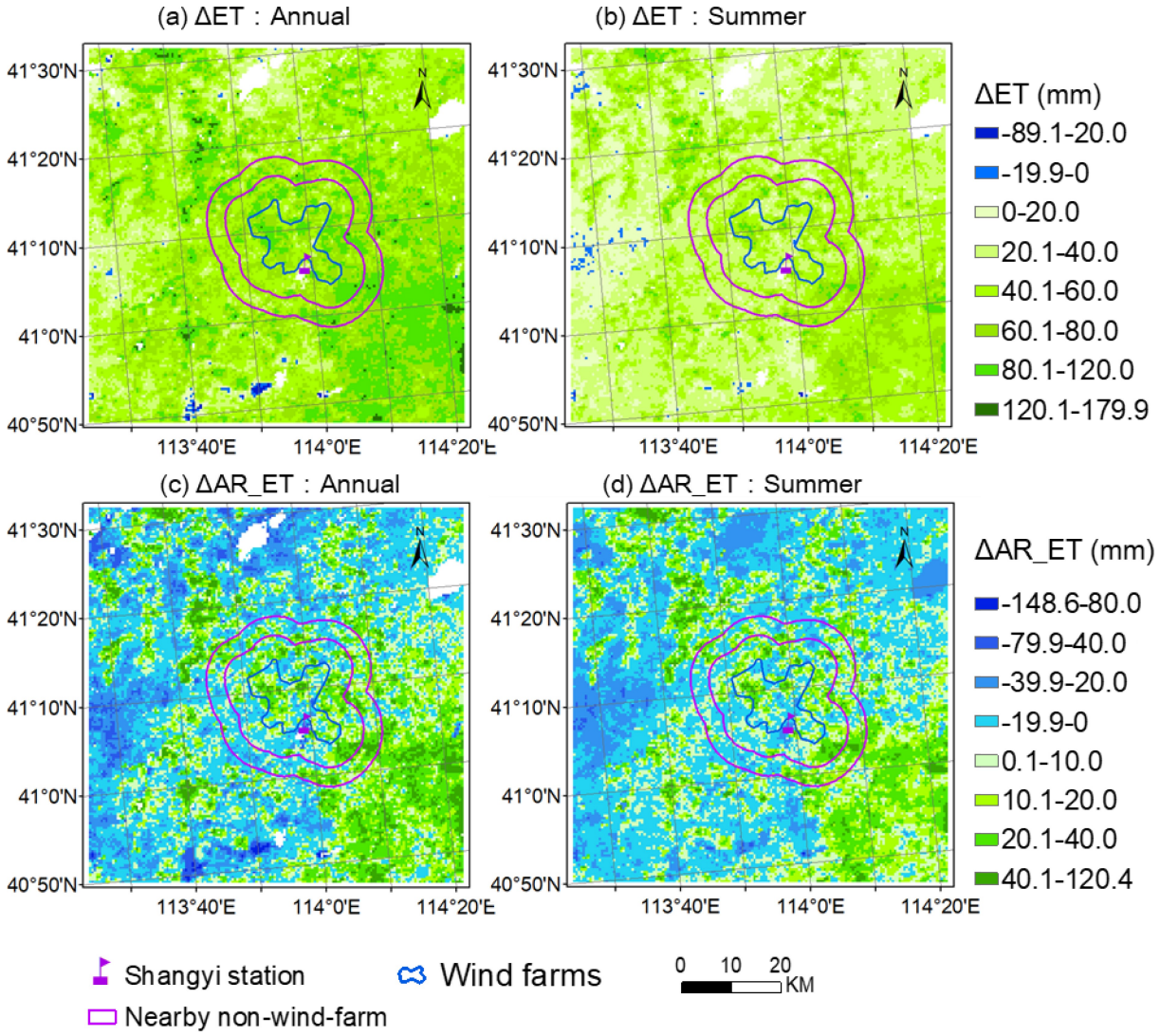

Fig. 7. Comparison of the changes in ET (ΔET) and the changes in ET regional anomalies (ΔAR_ET) after the wind farms were built (a) annual ΔET, (b) ΔET in summer, (c) annual ΔAR_ET, and (d) ΔAR_ET in summer.

The ΔDLST for different periods such as annual, annual daytime, annual nighttime, summer nighttime, and winter nighttime were all within ±0.1°C, i.e., smaller than their interannual fluctuations (0.05°C–0.57°C) during the preconstruction period. Thus, this observation indicates that there was no significant increase in the LST in the wind farms area, and in contrast, both the annual mean LST and annual mean daytime LST were slightly lowered.

The ΔDET values throughout the year and summer were 2.75 mm and 0.15 mm, respectively, which indicates that despite the slight increase in ET, both values were smaller than their corresponding interannual fluctuations during the preconstruction period (4.74 mm and 4.11 mm, respectively), which indicated that compared with the surrounding non-impacted areas, the ET changes in the wind farms were not obvious.

5. Discussion

5.1. *Effect of vegetation coverage on climate factors*

A previous study (Qiu et al., 2020) showed that ET variations in arid and semiarid areas are largely affected by changes in vegetation coverage, and ET is positively correlated with the NDVI. In the last 20 years, China has continuously carried out the "Natural Forest Resource Protection Project", the "Three North Shelterbelt Project", and the "Beijing–Tianjin Sandstorm-source Control Project", leading to an increase in vegetation coverage in this area (Li et al., 2019), including the research area of our study. Figure 9a illustrates the change in the NDVI between the pre-and post-construction periods, which is one of the important proxies for tracing variations in vegetation coverage. This fig-

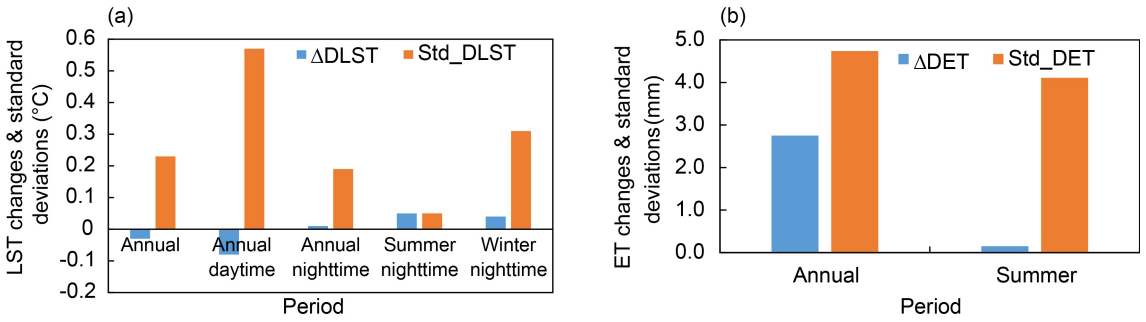

Fig. 8. Comparison of the changes in LST (a) and ET (b) after wind farm construction for different time periods and their internnual standard deviations before the construction of the wind farms. ΔDLST and ΔDET are the local changes in the LST anomaly and ET, respectively, between the wind farms area and the non-impacted area after the construction of the wind farms (2016–18), and Std_DLST and Std_DET are the interannual standard deviations of LST anomaly and ET anomaly, respectively, before the construction of the wind farms (2003–08).

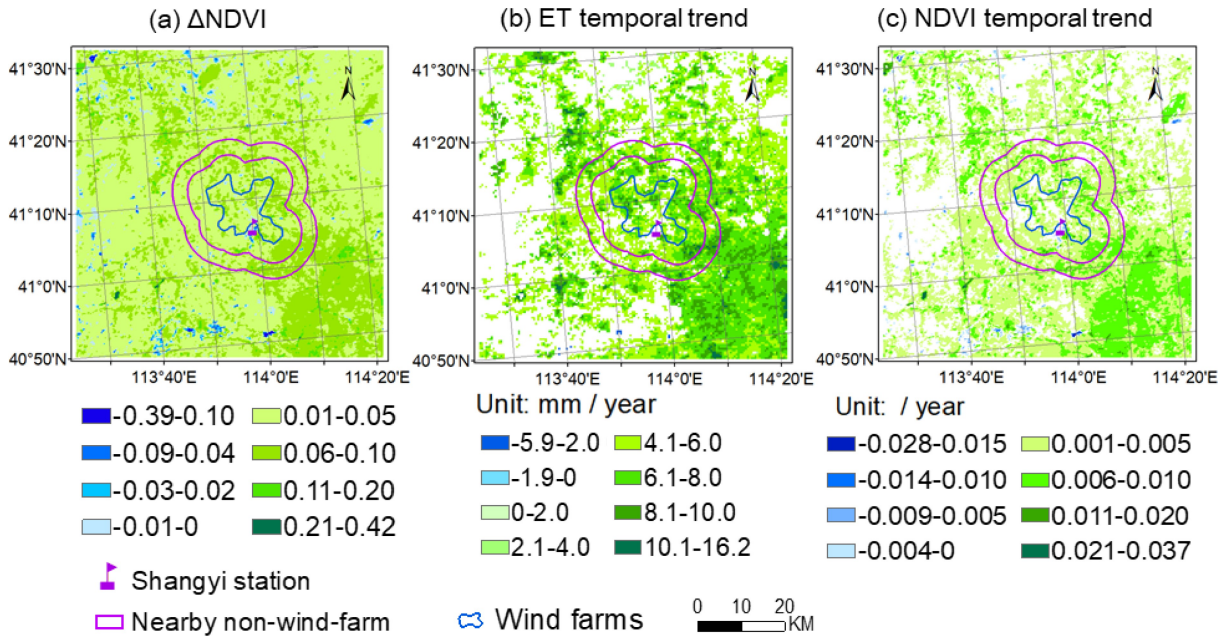

Fig. 9. Changes in NDVI (ΔNDVI) after the wind farms were built (a), and the temporal trend in ET (b), and temporal trend in NDVI (c) for the SWF and surrounding areas during 2003–18. The areas with values for the temporal trends in NDVI and ET indicate that the trend passed the 95% confidence level, and the blank area indicates that there was no significant trend of change.

ure shows that after the wind farms were built, the NDVI was enhanced in both the area of the wind farm as well as the entire region, indicating that the difference in vegetation coverage did not result from the local wind farms. ET and the NDVI in the majority of the region increased during 2003–18 (Figs. 9b, c) and were spatially well correlated. In addition, a positive correlation between the NDVI and ET in the wind farms area was identified during 2003–18 (Fig. 10a), with a Pearson correlation coefficient of 0.81. As shown by the linear regression fit, the change in the NDVI explained 65% of the change in ET. The above analysis indicates that the increase in ET in the wind farms area was mainly caused by the higher NDVI resulting from the increased vegetation coverage.

Similarly, changes in vegetation coverage influence LST changes. In semiarid prairies, when the NDVI increases, the LST decreases (Shuai et al., 2018). A negative correlation exists between the NDVI and LST in the wind farms area during 2003–18 (Fig. 10b), with a Pearson correlation coefficient of –0.65. Thus, the increase in the NDVI in the wind farms area perhaps induced a corresponding reduction in the LST, which canceled out the increasing effect of the wind farms on the LST.

In arid and semiarid areas, the vegetation coverage and relative humidity are positively correlated (Zhang et al. 2019). Wind farms generally reduce relative humidity due to local heating effects (Hu, 2012; Xu, 2014), which is inconsistent with the increase in the rH from the meteorological observation in Fig. 5c. To explore the reasons for the increase, an anomaly calculation was carried out between the NDVI within the wind farms area and the NDVI within five kilometers around the Shangdu station from 2003–18. The Pearson correlation between the NDVI anomaly and the rH during 2003–18 was 0.65, which indicated that the increase in the rH was perhaps due to the enhanced NDVI. In addition, the absolute values of the Pearson correlation coefficients between the NDVI anomaly and the ΔT, rW, and rP during 2003–18 were all below 0.3, which showed that the changes in NDVI had little impact on air temperature, wind speed, and precipitation.

5.2. *Comparison with regional climate change*

The air temperature increase in the wind farms area observed in this study was 0.37°C, which is higher than the interannual fluctuation (0.13°C). In addition, the 0200 LT air temperature increase was close to 1°C, which highlights a significant and unignorable rise in the local air temperature. However, when compared with changes in the regional climate, this enhancement is smaller than observed long-term air temperature variations in North China. The annual mean air temperature has been rising at a rate of 0.40°C per decade during 1981–2017, and the air temperature in 2018 was approximately 0.60°C higher than in 2003 (North China Regional Climate Change Assessment Report Writing Committee, 2021). In addition, the annual mean wind speed in the wind farms area is only 6% lower from 2003–18, which is slightly higher than its natural interannual fluctuation (5%) and lower than observed long-term wind speed variations in North China. The annual average wind speed has been decreasing at a rate of 0.13 m s^{-1} per decade during 1981–2017, and the wind speed in 2018 was approximately 7.5% lower than in 2003 (North China Regional Climate Change Assessment Report Writing Committee, 2021). This evidence strongly suggests that the SWF had no significant impact on the regional climate. These findings are in good agreement with the conclusions of Wang et al. (2019) in the numerical simulation of the Zhangbei Wind Farm in Hebei Province, another wind farm in Zhangjiakou. We may therefore conclude that the impact of substantial wind farms on the local area is significant, while the impact on the regional area is slight.

5.3. *Comparison with other results*

In this study, based on meteorological observations, we further confirm that the atmosphere warming effect mainly occurred at nighttime in summer and autumn, in good agreement with previous findings based on the LST data from satellite observations that the land surface temperature enhancement effect mainly occurs at nighttime in summer and autumn (Zhou et al., 2013a; Chang et al., 2016). However, the air temperature increases (0.37°C in the annual mean air temperature and 0.37°C–0.95°C in the 0200 LT air temperature) obtained in this study are higher than most of the previously reported values. For instance, Armstrong et al. (2016) observed a 0.18°C increase at night in a wind farm area and Zhang et al. (2019) observed a 0.24°C increase in the

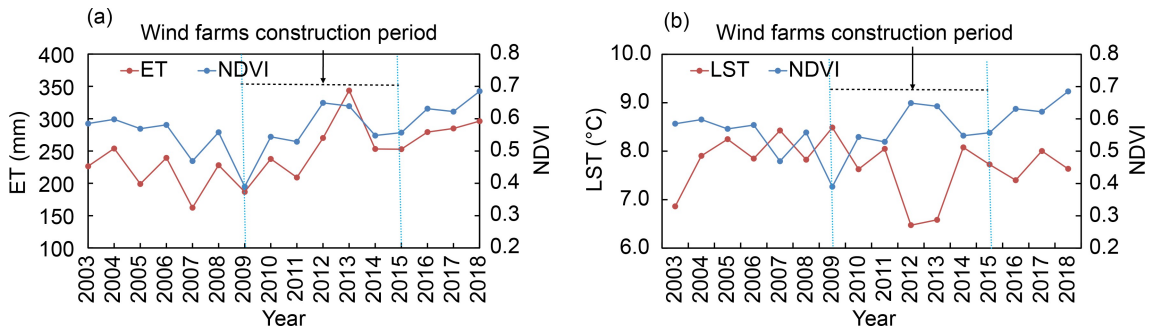

Fig. 10. Comparison of the interannual variations of ET and NDVI (a), and LST and NDVI (b) for the SWF from 2003 to 2018. *R* is the Pearson correlation coefficient.

annual mean air temperature in a wind farm area in the Dabie Mountains. The air temperature enhancement effect observed at the SWF in this study also exceeds both the increases in nighttime LST (0.31°C–0.71°C) observed at large-scale wind farms in central and western Texas, USA, based on MODIS satellite data (Zhou et al., 2013a) and the observed increases in nighttime LST (0.38°C–0.51°C) at wind farms in Guazhou, Gansu Province, China (Chang et al., 2016). Our studied wind farms have only 257 wind turbines and cover an area of only about 200 km^2. It is much smaller than the large-scale wind farms in central and western Texas (2358 wind turbines, approximate area of 2000 km^2) and the wind farms in Guazhou, Gansu Province, China (>1000 wind turbines, approximate area of 1000 km^2). These facts together suggest that local air temperature enhancements in the wind farms area probably are not correlated with the size of the wind farms. It may be related to the climate type, and further research is needed.

In the wind farms area, the 0200 LT air temperature decreased significantly (–0.36°C) in spring and decreased slightly (–0.02°C) in the autumn. This finding is consistent with the observation results from a wind farm in San Gorgonio, California (Roy and Traiteur 2010), and similar results have been simulated by numerical approach (Vautard et al., 2014; Wang et al., 2019). It may be explained by the cooling effect of a negative vertical air temperature gradient during the day in the wind farms (Roy and Traiteur, 2010). During the daytime, the near-surface air has a decreasing stratification and is in an unstable state, i.e., cold air lying above warm air. The rotation of wind turbines promotes vertical mixing, and in turn, cold air moves downward and warm air moves upward, thus leading to a cooling effect during the daytime. This cooling effect, however, is absent in summer and autumn at 1400 LT (Fig. 5a). Thus, more observations from other aspects are needed to further analyze the impact of wind farms on the near-surface air temperature during daytime and the mechanisms related to this impact.

This study verifies from field observation that wind farms in Zhangjiakou are responsible for the observed reduction in wind speed, which differs from the conclusions of previous studies of the effects on the wind speed of wind farms in Zhangjiakou (Huo et al., 2015; Li et al., 2015; Yan et al., 2015). The discrepancy may be caused by two factors. First, the meteorological stations used in previous work do not lie within the impact range of the wind farms of interest. Second, regarding research scales, this study focused mainly on a local scale, i.e., the wind farms area, while previous studies focused on large-scale areas, the finding of no impact on a regional scale can be consistently explained if the impact of wind farms is constrained to the local area.

5.4. *Some uncertainties*

The selected background weather station probably does not truly reflect the background climate where the wind farm is located and thus cannot completely eliminate interannual and climate changes that have occurred at the SY station. For example, the correlation coefficient for the annual mean wind speed between the SY station and SD station is less than 0.8 (Fig. 2a), which leads to some uncertainty regarding the wind speed changes due to the wind farms. Therefore, due to the large interannual variability of various climatic elements of the SY and SD stations, the analysis of temporal variations for different climate factors has a degree of uncertainty. For example, the temporal change of the wind speed ratio between the SY and SD stations during 1997–2003 (Fig. 3d) and the abrupt change point of the wind speed ratio in 1996 (Fig. 4b), both unrelated to wind farms, increase the uncertainty that wind farms are significantly affecting wind speed. Therefore, further scientific observation experiments are needed to determine the quantitative impact of wind farms on wind speed.

The observation time after the construction of the wind farms is short (less than 10 years), and only three years are analyzed for the post-construction states. Due to a lack of long-term statistical support, there are some uncertainties regarding the changes in local climate factors after the construction of the wind farms. In the future, observational data spanning a longer time period after the construction of the wind farms will be needed to verify and revise the research conclusions of this paper.

6. Conclusions

This paper investigated the local climate effects [air temperature, wind speed, relative humidity, precipitation, land surface temperature (LST), and evapotranspiration (ET)] of the SWF in Zhangjiakou, Hebei Province, China. The impact of vegetation coverage changes of wind farms on local climate factors was also analyzed. The results showed that after the construction of the wind farms, the annual mean air temperature increased by 0.37°C in the wind farms area, with this increase occurring primarily at night especially in summer and autumn (0.95°C and 0.93°C, respectively). The daytime temperature changes were marginal, and their signs varied depending on the season. The annual wind speed dropped by 6%, which was mainly driven by decreases in spring and winter of 14% and 8%, respectively. The wind farms had no impact on the annual precipitation. The increase in NDVI may be an important reason for the increase in relative humidity. The increase in ET in the wind farms based on satellite observations was very likely caused by the enhanced NDVI, and that the lack of increased LST could have resulted from the increased NDVI canceling out the increase in the LST caused by the wind farms. Our results confirm the local atmospheric warming and wind speed reduction effects of wind farms in Zhangjiakou and furthermore suggest that the impact of wind farms on the regional climate is slight, which is of reference significance for the future development of wind power in this region.

Acknowledgements. This research was supported by the National Key R&D Program of China (2018YFB1502801). We thank the anonymous reviewers for their valuable comments.

REFERENCES

Abbasi, S. A., Tabassum-Abbasi, and T. Abbasi, 2016: Impact of wind-energy generation on climate: A rising spectre. *Renewable and Sustainable Energy Reviews*, **59**, 1591–1598, https://doi.org/10.1016/j.rser.2015.12.262.

Armstrong, A., R. R. Burton, S. E. Lee, S. Mobbs, N. Ostle, V. Smith, S. Waldron, and J. Whitaker, 2016: Ground-level climate at a peatland wind farm in Scotland is affected by wind turbine operation. *Environmental Research Letters*, **11**(4), 044024, https://doi.org/10.1088/1748-9326/11/4/044024.

Cervarich, M. C., S. B. Roy, and L. M. Zhou, 2013: Spatiotemporal structure of wind farm-atmospheric boundary layer interactions. *Energy Procedia*, **40**, 530–536, https://doi.org/10.1016/j.egypro.2013.08.061.

Chang, R., R. Zhu, and P. Guo, 2016: A case study of land-surface-temperature impact from large-scale deployment of wind farms in China from Guazhou. *Remote Sensing*, **8**(10), 790, https://doi.org/10.3390/rs8100790.

Chen, Z. H., F. He, Y. Cui, and X. T. Zhang, 2018: Advances in research of influence on climate of the group of wind farms in past 20 years. *Climate Change Research*, **14**(4), 381–391, https://doi.org/10.12006/j.issn.1673-1719.2017.009. (in Chinese with English abstract)

Christiansen, M. B., and C. B. Hasager, 2005: Wake effects of large offshore wind farms identified from satellite SAR. *Remote Sensing of Environment*, **98**(2–3), 251–268, https://doi.org/10.1016/j.rse.2005.07.009.

Fitch, A. C., 2015: Climate impacts of large-Scale wind farms as Parameterized in a global climate model. *J. Climate*, **28**(15), 6160–6180, https://doi.org/10.1175/JCLI-D-14-00245.1.

Fitch, A. C., J. K. Lundquist, and J. B. Olson, 2013: Mesoscale influences of wind farms throughout a diurnal cycle. *Mon. Wea. Rev.*, **141**, 2173–2198, https://doi.org/10.1175/MWR-D-12-00185.1.

Frandsen, S. T., and Coauthors, 2009: The making of a second-generation wind farm efficiency model complex. *Wind Energy*, **12**, 445–458, https://doi.org/10.1002/we.351.

GWEC, 2020: Global wind energy report. Global Wind Energy Council. [Available online from https://www.geidco.org/2020/0403/2136.shtml]

Harris, R. A., L. M. Zhou, and G. Xia, 2014: Satellite observations of wind farm impacts on nocturnal land surface temperature in Iowa. *Remote Sensing*, **6**, 12 234–12 246, https://doi.org/10.3390/rs61212234.

Hu, J, 2012: Numerical simulation research on impact of large-scale wind farms on regional climate. M.S. thesis, Lanzhou University, 1–47.

Hu, J., and S. Wang, 2018: Impact of large-scale wind power base located in Gansu Jiuquan on regional climate. *Journal of Global Energy Interconnection*, **1**(2), 120–128, https://doi.org/10.3969/j.issn.2096-5125.2018.02.004. (in Chinese with English abstract)

Huo, L. F., Y. L. Zhou, and C. J. Li, 2015: Correlation analysis of wind farm construction and wind velocity in Zhangjiakou city. *Journal of Hebei North University* (*Natural Science Edition*), **31**(6), 60–63, https://doi.org/10.3969/j.issn.1673-1492.2015.06.015. (in Chinese with English abstract)

Jiang, J. X., L. W. Yang, Z. C. Li, and X. Q. Gao, 2019: Progress in the research on the impact of wind farms on climate and environment. *Advances in Earth Science*, **34**(10), 1038–1049, https://doi.org/10.11867/j.issn.10018166.2019.10.1038. (in Chinese with English abstract)

Leung, D. Y. C., and Y. Yang, 2012: Wind energy development and its environmental impact: A review. *Renewable and Sustainable Energy Reviews*, **16**(1), 1031–1039, https://doi.org/10.1016/j.rser.2011.09.024.

Li, C. J., L. F. Huo, and L. J. Niu, 2015: Analysis of the impact of wind power on wind speed in Zhangjiakou. *Journal of Hebei Institute of Architecture and Civil Engineering*, **33**(3), 105–109, https://doi.org/10.3969/j.issn.1008-4185.2015.03.028. (in Chinese with English abstract)

Li, G. Q., Z. F. Liu, X. L. Chang, and M. Zhang, 2016: Effects of wind farms on grassland regional surface evapotranspiration. *Ecological Science*, **35**(6), 146–151, https://doi.org/10.14108/j.cnki.1008-8873.2016.06.020. (in Chinese with English abstract)

Li, W., H. Z. Gong, H. K. Zang, J. H. Li, and X. F. Zhang, 2018: Research progress on the Impact of wind farms on regional and global climate. *Environmental Protection*, **46**(3), 69–73, https://doi.org/10.14026/j.cnki.0253-9705.2018.z1.013. (in Chinese with English abstract)

Li, Y. H., J. H. Teng, and W. T. Ma, 2019: Temporal and spatial evolution characteristics of vegetation coverage in Beijing-Tianjin-Hebei region. *Beijing Surveying and Mapping*, **33**(11), 1302–1307, https://doi.org/10.19580/j.cnki.1007-3000.2019.11.003. (in Chinese with English abstract)

Mu, Q. Z., M. S. Zhao, and S. W. Running, 2011: Improvements to a MODIS global terrestrial evapotranspiration algorithm. *Remote Sens. Environ.*, **115**(8), 1781–1800, https://doi.org/10.1016/j.rse.2011.02.019.

North China Regional Climate Change Assessment Report Writing Committee, 2021: North China regional climate change assessment report in 2020: Summary of decision-makers. Meteorological Science Press, Beijing, 1–22. (in Chinese)

Qiu, L. S., L. F. Zhang, Y. He, Y. D. Chen, and W. H. Wang, 2020: Spatiotemporal Variations of Evapotranspiration and Influence Factors in Qilian Mountain from 2000 to 2018. *Research of Soil and Water Conservation*, **27**(3), 210–217, https://doi.org/10.13869/j.cnki.rswc.2020.03.031. (in Chinese)

Rajewski, D., and Coauthors, 2013: Crop wind energy experiment (CWEX): Observations of surfacelayer, boundary layer, and mesoscale interactions with a wind farm. *Bull. Am. Meteor. Soc.*, **94**, 655–672, https://doi.org/10.1175/BAMS-D-11-00240.1.

Roy, B. S., 2011: Simulating impacts of wind farms on local hydrometeorology. *Journal of Wind Engineering and Industrial Aerodynamics*, **99**(4), 491–498, https://doi.org/10.1016/j.jweia.2010.12.013.

Roy, S. S., 2004: Can large wind farms affect local meteorology? *J. Geophys. Res.*, **109**(D19), D19101, https://doi.org/10.1029/2004JD004763.

Roy, S. M., and J. J. Traiteur, 2010: Impacts of wind farms on surface air temperatures. *Proceedings of the National Academy of Sciences of the United States of America*, **107**(42), 17 899–17 904, https://doi.org/10.1073/pnas.1000493107.

Shuai, C., J. M. Sha, J. H. Lin, J. W. Ji, Z. L. Zhou, and S. Gao, 2018: Spatial difference of the relationship between remote sensing index and land surface temperature under different underlying surfaces. *Journal of Geo-Information Science*, **20**(11), 1657–1666, https://doi.org/10.12082/dqxxkx.2018.180303. (in Chinese with English abstract)

Smith, C. M., R. J. Barthelmie, and S. C. Pryor, 2013: In situ obser-

vations of the influence of a large onshore wind farm on near-surface temperature, turbulence intensity and wind speed profiles. *Environmental Research Letters*, **8**(3), 034006, https://doi.org/10.1088/1748-9326/8/3/034006.

Sun, H. W., Y. Luo, Z. C. Zhao, and R. Chang, 2018: The impacts of Chinese wind farms on climate. *J. Geophys. Res.*, **123**, 5177–5187, https://doi.org/10.1029/2017JD028028.

Vautard, R., F. Thais, I. Tobin, F. M. Bréon, J. G. Devezeaux de Lavergne, A. Colette, P. Yiou, and P. M. Ruti, 2014: Regional climate model simulations indicate limited climatic impacts by operational and planned European wind farms. *Nature Communications*, **5**, 3196, https://doi.org/10.1038/ncomms4196.

Walsh-Thomas, J. M., G. Cervone, P. Agouris, and G. Manca, 2012: Further evidence of impacts of large-scale wind farms on land surface temperature. *Renewable and Sustainable Energy Reviews*, **16**, 6432–6437, https://doi.org/10.1016/j.rser.2012.07.004.

Wan, Z. M., 2008: New refinements and validation of the MODIS land-surface temperature/emissivity products. *Remote Sens. Environ.*, **112**, 59–74, https://doi.org/10.1016/j.rse.2006.06.026.

Wang, C., and R. G. Prinn, 2009: Potential climatic impacts and reliability of very large-scale wind farms. *Atmospheric Chemistry and Physics Discussions*, **9**(5), 19 081–19 102.

Wang, Q., K. Luo, C. L. Wu, and J. R. Fan, 2019: Impact of substantial wind farms on the local and regional atmospheric boundary layer: Case study of Zhangbei wind power base in China. *Energy*, **183**, 1136–1149, https://doi.org/10.1016/j.energy.2019.07.026.

Wei, F. Y., 2007: *Modern Technology of St Atistics, Diagnosis and Forecast for Climate*. 2nd ed., China Meteorological Press, Beijing, 63–65. (in Chinese)

Xia, G., L. M. Zhou, J. M. Freedman, S. B. Roy, R. A. Harris, and M. C. Cervarich, 2016: A case study of effects of atmospheric boundary layer turbulence, wind speed, and stability on wind farm induced temperature changes using observations from a field campaign. *Climate Dyn.*, **46**(7–8), 2179–2196, https://doi.org/10.1007/s00382-015-2696-9.

Xu, R. H., 2014: The impact of wind farm on local micro meteorological environment in arid region—Taking Zhurihe wind farm as an example. M.S. thesis, Inner Mongolia Agricultural University, 1–64. (in Chinese)

Yan, L., Y. G. Li, and X. Zhao, 2015: Research on the impact of wind power development on the formation of heavy smog in Beijing-Tianjin-Hebei. *Liaoning Urban and Rural Environmental Science & Technology*, **35**(9), 67–71, https://doi.org/10.3969/j.issn.1674-1021.2015.09.020. (in Chinese)

Zhang, X. T., J. X. Li, Z. H. Chen, F. He, and Y. Cui, 2019: A preliminary exploration on the influence of wind farms on local climate in Dabie Mountainous areas in China: A case study of Dawu in Hubei province. *Advances in Meteorological Science and Technology*, **9**(2), 56–61, https://doi.org/10.3969/j.issn.2095-1973.2019.02.011. (in Chinese with English abstract)

Zhao, Z. C., Y. Luo, and Y. Jiang, 2011: Advances in assessment on impacts of wind farms upon climate change. *Advances in Climate Change Research*, **7**(6), 400–406, https://doi.org/10.3969/j.issn.1673-1719.2011.06.003. (in Chinese with English abstract)

Zhou, L. M., Y, H. Tian, S. B. Roy, C. Thorncroft, L. F. Bosart, and Y. L. Hu, 2012: Impacts of wind farms on land surface temperature. *Nature Climate Change*, **2**(7), 539–543, https://doi.org/10.1038/nclimate1505.

Zhou, L. M., Y. H. Tian, S. B. Roy, Y. J. Dai, and H. S. Chen, 2013a: Diurnal and seasonal variations of wind farm impacts on land surface temperature over western Texas. *Climate Dyn.*, **41**(2), 307–326, https://doi.org/10.1007/s00382-012-1485-y.

Zhou, L. M., Y. H. Tian, H. S. Chen, Y. J. Dai, and R. A. Harris, 2013b: Effects of topography on assessing wind farm impacts using MODIS data. *Earth Interactions*, **17**(13), 1–18, https://doi.org/10.1175/2012EI000510.1.

Zhu, R., 2014: Preliminary study on the impact of large-scale wind power development on urban air environmental pollution. *Wind Energy*(5), 48–53, https://doi.org/10.3969/j.issn.1674-9219.2014.05.025. (in Chinese with English abstract)